Human Lysozyme Possesses Novel Antimicrobial Peptides within Its N-terminal Domain that Target Bacterial Respiration

Hisham R. Ibrahim,* Kenta Imazato, and Hajime Ono

Department of Biochemistry and Biotechnology, Faculty of Agriculture, Kagoshima University, Kagoshima 890-0065, Japan

ABSTRACT: Human milk lysozyme is thought to be a key defense factor in protecting the gastrointestinal tract of newborns against bacterial infection. Recently, evidence was found that pepsin, under conditions relevant to the newborn stomach, cleaves chicken lysozyme (cLZ) at specific loops to generate five antimicrobial peptide motifs. This study explores the antimicrobial role of the corresponding peptides of human lysozyme (hLZ), the actual protein in breast milk. Five peptide motifs of hLZ, one helix−loop−helix (HLH), its two helices (H1 and H2), and two helix−sheet motifs, H2−β-strands 1−2 (H2−S12) or H2−β-strands 1−3 (H2−S13), were synthesized and examined for antimicrobial action. The five peptides of hLZ exhibit microbicidal activity to various degrees against several bacterial strains. The HLH peptide and its N-terminal helix (H1) were significantly the most potent bactericidal to Gram-positive and Gram-negative bacteria and the fungus *Candida albicans*. Outer and inner membrane permeabilization studies, as well as measurements of transmembrane electrochemical potentials, provided evidence that HLH peptide and its N-terminal helix (H1) kill bacteria by crossing the outer membrane of Gram-negative bacteria via self-promoted uptake and are able to dissipate the membrane potential-dependent respiration of Gram-positive bacteria. This finding is the first to describe that hLZ possesses multiple antimicrobial peptide motifs within its N-terminal domain, providing insight into new classes of antibiotic peptides with potential use in the treatment of infectious diseases.

KEYWORDS: lysozyme, breast milk, antimicrobial peptides, helix motifs, innate immune, membrane potential, bacterial respiration, antibiotic peptides, peptide therapy

INTRODUCTION

Lysozyme is an antimicrobial protein widely distributed in various biological fluids and tissues, including avian egg and animal secretions, human milk, tears, saliva, and airway secretions, and is secreted by polymorphonuclear (PMN) leukocytes.[1] It belongs to a class of enzymes that lyse the cell walls of certain Gram-positive bacteria, as it splits the bond between *N*-acetylglucosamine and *N*-acetylmuramic acid of the peptidoglycan in the bacterial cell walls. Besides its antimicrobial activity, lysozyme has many other functions including inactivation of viruses,[2,3] important roles in surveillance of membranes of mammalian cells, enhancement of phagocytic activity of macrophages, and stimulation of proliferation and antitumor functions of monocytes.[4−6] The in vitro antimicrobial activity of lysozyme is directed against certain Gram-positive bacteria and, to a lesser degree, against Gram-negative bacteria.[7,8] The active role played by lysozyme in defense systems against bacterial infections to the epithelia of the respiratory organs and gastrointestinal tract has long been recognized.[2,7,10,11] However, the molecular mechanism for the antimicrobial function of lysozyme remained unclear until our recent finding that chicken lysozyme (cLZ) possesses antimicrobial activity independent of its catalytic function and appears to depend on a structural phase transition in the molecule.[2,7,10−14]

The lysozyme molecule consists of two domains, α and β, between which the active site is located.[9] With computer-aided analysis, we found a helix−loop−helix (HLH) located at the upper lip of the active site cleft of chicken and human lysozymes [residues 87−114 in cLZ and residues 87−115 in human lysozyme (hLZ)] with a broad spectrum of bactericidal activity.[15] The distribution and number of genes that encode lysozyme vary considerably among species.[16] The cellular source of lysozyme includes PMN leukocytes, monocytes, macrophages, keratinocytes, Paneth cells of the small intestine, epithelial cells of trachea, pneumocytes, and secretory cells of the apocrine gland.[17−22] In humans, lysozyme is secreted in tears, saliva, amniotic fluid, and, abundantly, in breast milk.[1,10] The physiological fluids in which lysozyme is known to exert its defense role against bacterial infections suggest a protease-dependent strategy by which its antimicrobial action is modulated in vivo. For instance, the lysosomal aspartic proteases of azurophil granules, including cathepsin D, have been reported to potentiate the antimicrobial activity of lysozyme against Gram-negative bacteria.[23] Tear and saliva components, which play a role in defense against infections, include cathepsins G and D.[24−28] Furthermore, the presence of cathepsin D in milk has recently been reported.[24] Human milk contains a significant amount of lysozyme and seems to play a major role in the local protection of infant's gastrointestinal tract.[29,30] While developing the immune system, the breast-fed neonate is provided with 0.3−0.5 g/L of lysozyme via the milk.[31] In parallel, the stomach is well-known for its secretion of pepsin A, a member of the aspartic protease family, secreted predominantly by chief cells in the gastric mucosa. Aspartic proteases, such as pepsin A, rennin, cathepsins D and E, and embryonic pepsin, are involved in several severe pathologies of the gastrointestinal mucosa, including bacterial infections and cancer.[32−36]

In an attempt to elucidate the functional significance of the distinct coexistence of lysozyme with aspartic proteases on the molecular mechanism of its antimicrobial action, we recently found that pepsin, under conditions relevant to the newborn stomach, generates a complex of antimicrobial peptide motifs (helical, helix—loop—helix, and helix—sheet) originated from the N-terminus of chicken lysozyme.[37] Five bactericidal peptides corresponding to amino acid residues 1—17 (helix-1), 21—38 (helix-2), 1—38 (helix1—loop—helix-2), 21—56 (helix-2—strands 1—2), and 21—62 (helix-2—strands 1—3) of chicken lysozyme were identified. Our sequence alignment of lysozymes from different species, particularly hLZ, indicated that they possess putative cleavage sites by pepsin at pH 4.0 at almost similar positions found in chicken lysozyme. It is likely that proteolytic processing, by pepsin in the newborn stomach or by cathepsin D in the azurophil granules, is a key biological process producing an array of peptides with different activities from hLZ. Whether these peptides, assumed to be released by neonate pepsin, contribute to the antimicrobial action of hLZ is yet to be unraveled. The pursuit of these peptides could be linked to the hope that synthetic or recombinant derivatives of antibiotic peptides from hLZ may have a future as administered agents for the treatment of infection and its sequelae.

This study was undertaken to unravel the peptide-based bactericidal action of hLZ, particularly to elucidate the antimicrobial role of the individual peptides of hLZ assumed to be liberated upon cleavage with neonate pepsin. For this, the corresponding five peptides of hLZ were synthesized and tested for antimicrobial activity against different microorganisms. The synthetic peptides were also evaluated with regard to their ability to affect the integrity and potential of bacterial membranes. The importance of these highly conserved sequence motifs for antimicrobial specificity, the mechanism of action of hLZ, and their potential as new peptides antibiotic against bacterial infectious diseases are discussed.

■ MATERIALS AND METHODS

Materials. Human milk lysozyme (hLZ), 1-*N*-phenylnaphthylamine (NPN), 5,6-carboxyfluorescein diacetate (cFDA), 2′,7′-dichlorodihydrofluorescein diacetate (DCFH-DA), nigericin (Nig), 3,3′-diisopropylthiadicarbocyanine iodide (diS-C$_3$-5), and *O*-nitrophenyl-*β*-ᴅ-galactopyranoside (ONPG) were from Sigma-Aldrich (Tokyo, Japan). Valinomycin (Val) was from Wako Pure Chemicals (Osaka, Japan). Brain—heart infusion (BHI) broth and nutrient agar were from Difco Laboratories (Detroit, MI). Trypticase soy broth (TSB) was from Becton Dickinson (Tokyo, Japan). A TSK gel ODS-120T column for reversed-phase HPLC was from Tosoh (Tokyo, Japan). All other reagents were of analytical grade.

Microorganisms. Test microorganisms for antimicrobial assays, *Escherichia coli* K-12 (IFO 3301) and *Staphylococcus aureus* (IFO 14462), were obtained from the Institute of Fermentation (Osaka, Japan). *Corynebacterium minutissimum* (NBRC 15361) was from Nite Biological Resource Center (Tokyo, Japan). *Klebsiella pneumoniae* (ATCC 13883), *Staphylococcus epidermidis* (ATCC 12228), *Pseudomonas aeruginosa* (ATCC 27853), *Salmonella typhimurium* (ATCC 14028), *Propionibacterium acnes* (ATCC 6919), and the fungus *Candida albicans* (ATCC 2091) were from the American Type Culture Collection (Rockville, MD). Wild strains of *Bordetella bronchiseptica* and *Streptococcus zooepidemicus* were obtained from the Institute of Bacteriology of the Veterinary Hospital, Zürich, Switzerland.

Synthesis of Peptides. The peptides of hLZ, KVFERCELART-LKRLGM, RGISLANWMCLAKWESGY, KVFERCELARTLKRLGM-

DGYRGISLANWMCLAKWESGY, RGISLANWMCLAKWESGYN-TRATNYNAGDRSTDYGIF, and RGISLANWMCLAKWESGYNT-RATNYNAGDRSTDYGIFQINSRYW, were synthesized by Gen-Script Corp. (Piscataway, NJ). Peptides were further purified by reversed-phase HPLC using a TSK gel ODS 120 T column (7.8 mm × 300 mm, Tosoh, Tokyo, Japan) with a linear gradient (2—60% for 80 min) of acetonitrile containing 0.1% TFA, and the eluate was monitored at 214 nm. The pure peptides were collected, vacuum-dried, and used in the subsequent experiments. Fractions after HPLC separation were examined by using a Q-STAR XL LC/MS/MS system (Applied Biosystems, Tokyo, Japan).

Mass Spectrometry (MS/MS). The peptide fractions from reversed-phase HPLC in acetonitrile containing 0.1% TFA were lyophilized and added to 20 *μ*L of 0.1% formic acid. The mass spectra of peptides were detected with QSTAR Pulsar *i* LC-MS/MS (Applied Biosystems). Typically, 1000 V was applied to the spraying capillary. The range of total ion current was *m/z* 1—2000. The mass spectrometer was set to MS/MS mode.

Tricine-SDS-PAGE. Peptides were resolved on tricine-SDS-PAGE (16.5% gels) using 10 *μ*g of peptide/lane. The peptide bands were visualized by Coomassie Brilliant Blue R-250 (CBB), and the patterns were analyzed by gel scanning using an Electrophoretic Documentation and Analysis System 120 (EDAS 120) equipped with a DC120 Camera and Kodak ID 2.02 image analysis software (Eastman Kodak Co., Rochester, NY). The molecular sizes of species were estimated using peptide molecular weight standard (Bio-Rad, Hercules, CA).

Antimicrobial Activity. The bactericidal assay was performed as previously described.[15] Briefly, midlogarithmic phase cells, grown in BHI broth, were washed and resuspended (2 × 10^7 cells/mL) in TSB (pH 7.4). Aliquots (100 *μ*L) of each bacterial suspension were mixed with 100 *μ*L of 1% TSB containing the test peptide in 2-fold serial dilutions. Controls were incubated in the absence of peptide. The mixture was incubated at 37 °C for 2 h, serially diluted in physiological saline solution, and plated on nutrient agar. The colony-forming units (CFU) were obtained after incubation of the agar plates at 37 °C for 18 h.

Candidacidal Assay. The susceptibility of *C. albicans* was tested essentially according to the procedure described above for the antibacterial assay. Briefly, 50 *μ*L of 10^6 cfu/mL of *C. albicans* blastoconidia derived from a 24 h culture in TBS was incubated with 50 *μ*L of the test peptide solution and 100 *μ*L of 2% TSB in phosphate buffer. After an incubation time of 2 h at 30 °C, the mixture was plated on TSB agar. The plates were incubated for 24—48 h at 30 °C, and the colonies were counted. Antimicrobial assays were performed in duplicate.

NPN-Based Outer Membrane Damage Assay. Outer membrane (OM) permeabilization of *E. coli* K-12 and *P. aeruginosa* was determined by measuring NPN uptake by bacteria using black fluoroplates and an automated real-time kinetics fluorometer (Fluoroskan Ascent FL; Labsystems, Helsinki, Finland), as described previously.[38] Bacteria grown to log-phase were collected, washed, and resuspended (10^8 cfu/mL) in 10 mM HEPES buffer (pH 7.2). Aliquots of bacterial suspension (100 *μ*L) were pipetted onto prewarmed fluoroplate wells to 37 °C, containing 100 *μ*L of 10 mM HEPES buffer, NPN (10 mM), and different concentrations of LZ, test peptides, or polymyxin B (as positive control). Controls contained buffer instead of test compounds. Fluorescence was monitored from four parallel wells per sample at excitation and emission of 355 and 405 nm, respectively. For each test compound, it was ascertained that, alone or with 10 mM NPN, there was no fluorescence increase compared to mere NPN in buffer. The results are expressed as NPN uptake factors calculated as a ratio of background-corrected (with value in the absence of NPN subtracted) fluorescence values of the bacterial suspension and of the buffer, respectively. Results are representative of three independent experiments in triplicate.

Propidium Iodide(PI)-Based Cytoplasmic Membrane Integrity Assay. The PI stain was used to assess membrane integrity of Gram-negative *E. coli* and Gram-positive *S. aureus*, as described previously.[39]
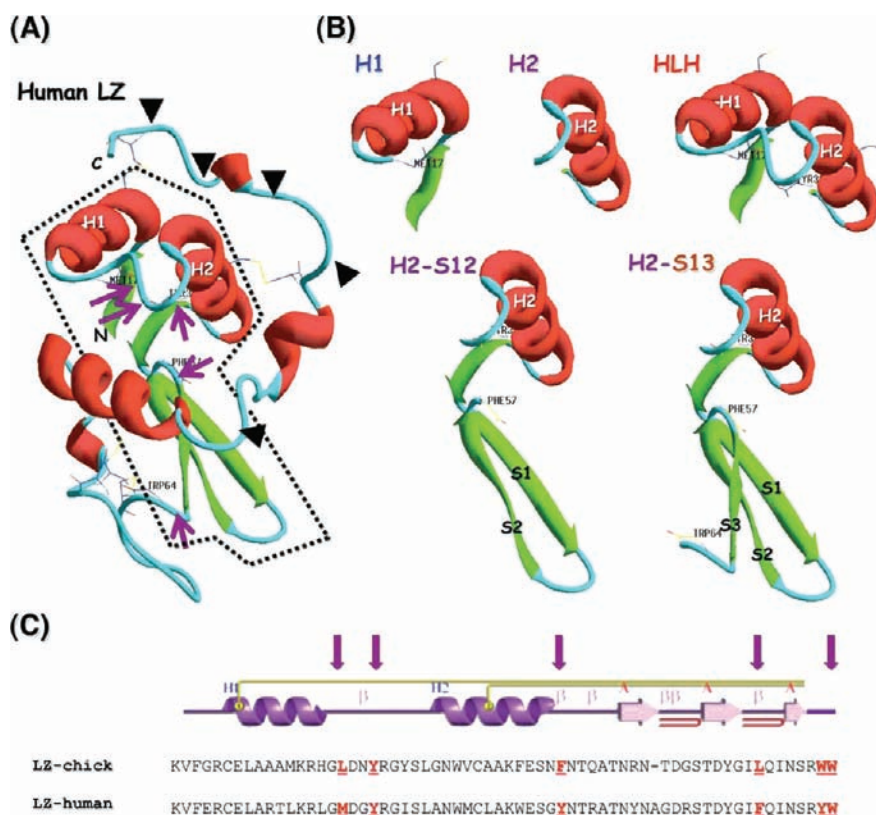
Figure 1. (A) Ribbon diagram of hLZ illustrating the predicted cutting sites by pepsin, which lies in loop regions that are aligned to release different peptide motifs from the N-terminal domain (boxed, dashed line). (B) Structures of the peptide motifs. Terminal residues are shown, and helix or β-strands are represented as H_n or S_n where n is the number within the molecule. (C) Sequence alignment of the N-terminal region of chicken and human lysozymes (LZ) demonstrating the conservation of amino acid residues sensitive to pepsin (bold, underlined). Arrows indicate the predicted sites for pepsin cleavage specificity.

Briefly, bacteria were grown in TSB to late log-phase, washed with 140 mM NaCl three times, and then diluted in NaCl to an OD at 670 nm of 0.03 for *E. coli* (10^8 cfu/mL) or 0.15 for *S. aureus* (10^7 cfu/mL). A mock treatment was set up with a total volume of 100 μL, containing mixtures of bacteria in NaCl with the PI dye mixture. Fluorescence emission was kinetically monitored for 60 min at 37 °C in Fluoroskan Ascent FL spectrofluorimeter at 620 nm with excitation at 544 nm. Another black fluoroplate containing a total volume of 100 μL per well of bacteria and increasing concentrations of peptides, hLZ, or polymyxin B was treated the same way as the mock treatment.

Transmembrane Electrical Potentials Assay. The effect of peptides on the transmembrane electrical potential ($\Delta\psi$m) of the Gram-positive *S. aureus* was determined using a modified version of the method described by Sims et al.[40] Briefly, 20 mL of bacterial culture was incubated at 37 °C until an OD_{675} of 0.6 was reached. The cells were then centrifuged at 5000g, washed, and resuspended in 200 μL of fresh TSB. The fluorescent probe 3,3′-dipropylthiadicarbocyanine iodide [$DiSC_3(5)$] was used to monitor the real-time kinetics changes in the $\Delta\psi$m of the cells. The fluorescence intensity of the probe was measured continuously at 25 °C in a 0.5 cm square cuvette thermostated using a JASCO FP-6600 fluorescence spectrophotometer (JASCO Corp., Tokyo), with excitation and emission wavelengths of 643 and 666 nm, respectively, and a slit width of 10 nm. Each cuvette contained 180 μL of 10 mM sodium phosphate buffer (pH 7.4), and 20 μL of the cell suspension in TSB. Next, the $DiSC_3(5)$ probe (5 μmol/L) was added to the system, resulting in a noticeable increase in the fluorescence of the probe. As the signal stabilized, the cells were spiked with 5 μmol of valinomycin to energize the $\Delta\psi$m; equilibration of the signal was

followed by addition of either 14 μM peptide or 2 μmol/L nigericin to collapse any remaining $\Delta\psi$m and to selectively reduce ΔpH. A negative control (Mock) contained distilled water instead of peptides.

Generation of Three-Dimensional (3D) Structures. Three-dimensional structures were generated by Swiss-PDB Viewer ver. 3.9 (Geneva Glaxo Welcome Experimental Research) using the Brookhaven PDB file of human lysozyme (1LZS). Sequence homology analysis was performed by MPsrch ver. 3.0, via the online BLITZ machine (European Molecular Biology Laboratory). Computation of the theoretical pI (isoelectric point) and M_w (molecular weight) of the synthetic peptides was performed on an ExPASy server, using Swiss-Prot sequence entries.

RESULTS

Design and Synthesis of the Peptide Motifs of Human Lysozyme. The proteolytic digestion of cLZ by pepsin, under conditions relevant to the newborn stomach, releases five antimicrobial peptides, whereas the cleavage occurred at conserved loops within the N-terminal domain.[37] The bactericidal peptides contained a HLH domain (residues 1−38), two α-helical peptides, generated from the HLH domain by nicking at leucine17, and two helix−sheet peptides consisting of the α-helix (residues 18−38) extended with either a two-stranded β-sheet (residues 39−56) or a three-stranded β-sheet (residues 39−60) structure. Figure 1 shows the 3D structure of hLZ and its domain (Figure 1A, boxed dashed line) from which pepsin is assumed to release the peptides (Figure 1B) corresponding to those of cLZ. The amino acid sequences of the full domain of cLZ and
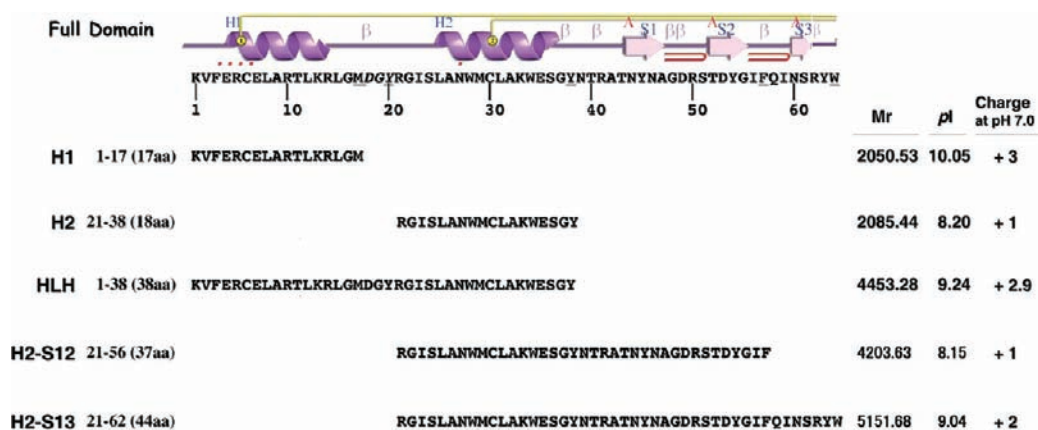
Figure 2. Amino acid sequences and designations of the synthetic peptides of hLZ investigated. Topology representation of the N-terminal domain is shown (top) illustrating the location and secondary structural elements of the synthetic peptides. The molecular masses (M_r) of the HPLC-purified peptides were confirmed by MS/MS analysis. Calculated pI and charge at pH 7.0 are shown.
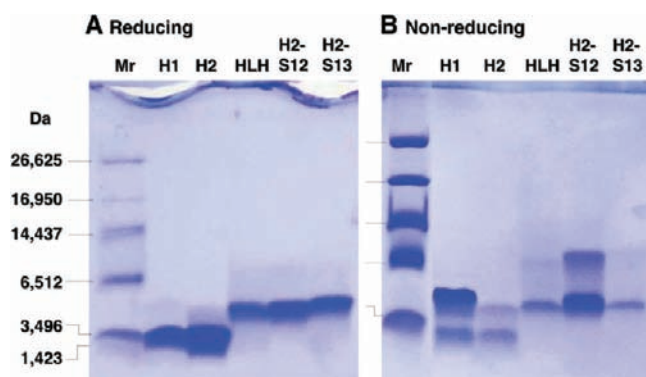
Figure 3. Tricine-SDS-PAGE analysis of the synthetic peptides of hLZ under reducing (A) and nonreducing (B) conditions. Under nonreducing conditions, peptides tend to form dimers, whereas H1 and H2—S12 exhibit the highest dimer-forming tendency (see text). Lane M_r shows peptide molecular weight markers in Da.

hLZ are shown in Figure 1C, whereas the domain falls within a region of greatest degree of conservation, particularly the five cleavage sites by pepsin (underlined residues), of both lysozymes.

The peptides could be classified as belonging to multiple peptide families, helix (H$_n$), HLH, and helix—sheet (H$_n$—S$_n$) families, where we have named individual peptides by using the letters H, L, and S to indicate α-helix, loop, and β-strand, respectively, and numbers (n) denote the order of the respective structure within the molecule. To closely examine the structural requirements and the antimicrobial action of these analogues, peptide motifs from hLZ, the full HLH peptide (residues 1—38), its N-terminal helix (H1, residues 1—17), its C-terminal helix (H2, residues 21—38), and the two helix—sheet peptides consisting of H2 extended with either the following two strands (H2—S12, residues 21—56) or three strands (H2—S13, residues 21—62) of hLZ were systematically synthesized (Figure 2).

Characterization of the Peptides. Molecular masses of the purified synthetic peptides of hLZ were analyzed by tricine-SDS-PAGE (Figure 3). Under reducing conditions (Figure 3A), the molecular masses of the five peptides were 2.0, 2.0, 4.4, 4.2, and 5.1 kDa, respectively, and MS/MS spectrometrical analysis confirmed their masses as 2050.53, 2085.44, 4453.28, 4203.63,

and 5151.68 Da, respectively (Figure 2). However, tricine-SDS-PAGE, under nonreducing conditions, identified H1, H2, and H2—S12 as peptides with high tendency to form dimers (Figure 3B), whereas the other peptides (HLH and H2—S13) were predominantly monomeric under either conditions. The results indicate that the cysteine residues within H1 (Cys-6) and H2 (Cys-30) may be involved in intermolecular disulfides in H1 and H2—S12, respectively, while forming an intramolecular disulfide (Cys6—Cys30) in HLH.
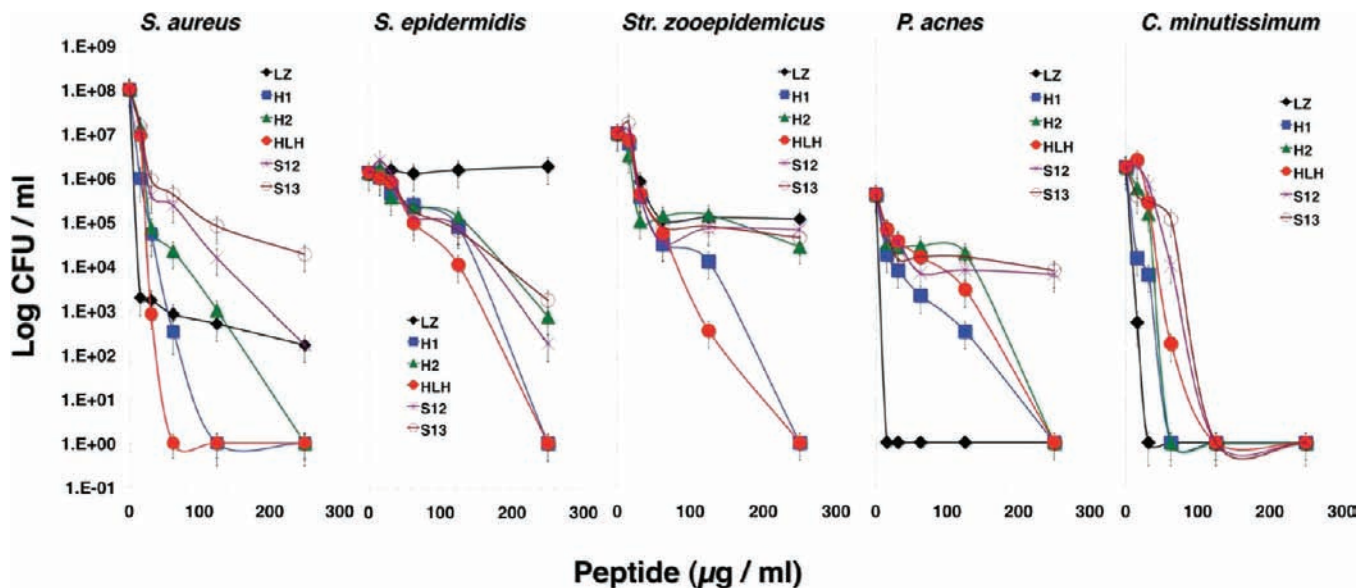
Bactericidal Activity of the Peptides. Human lysozyme and the synthetic peptides were tested for bactericidal activity against five Gram-negative (*E. coli*, *Salm. typhimurium*, *Bord. bronchiseptica*, *Kleb. pmeumonieae*, and *Ps. aeruginosa*) and five Gram-positive (*Staph. aureus*, *Staph. epidermidis*, *Str. zooepidemicus*, *Pr. acnes*, and *Co. minutissimum*) bacteria and a fungus (*Ca. albicans*). As shown in Figure 4, hLZ was devoid of activity against the Gram-negative *E. coli*, *Salm. typhimurium*, and *Bord. bronchiseptica* but exerted weak activity against *Kleb. pneumonieae* and *Ps. aeruginosa*. The bactericidal activity of the synthetic peptides was higher than that of hLZ against all Gram-negative bacterial strains investigated. However, HLH peptide exerted a markedly stronger bactericidal activity than the other peptides, followed by its derivative helics H1 and H2.

For the Gram-positive bacteria, human LZ showed no activity against *Staph. epidermidis* and weak activity against *Staph. aureus* and *Str. zooepidemicus* while exhibiting superior activity to all peptides against the skin pathogens *Pr. acnes* and *C. minutissimum* (Figure 5). The HLH peptide and its N-terminal helix (H1) were specifically bactericidal against *Staph. aureus*, *Staph. epidermidis*, and *Str. zooepidemicus* The C-terminal helix (H2) of the HLH was dose-dependently bactericidal, but to lesser degree than the HLH and H1, against all Gram-positive bacteria. The helix—sheet peptides (H2—S12 and H2—S13) were dose-dependently bactericidal, although to lesser degrees than the other peptides, against all Gram-positive bacteria except *Str. zooepidemicus*.

It is worth noting that the action of HLH peptide and its N-terminal helix (H1) was superior to that of other peptides against all strains tested, either the Gram-negative or Gram-positive bacteria. Although the five peptides exhibited significant fungicidal activity against *Ca. albicans*, the H1, H2, and H2—S12 peptides were virtually superior to the parent HLH and H2—S13, whereas hLZ exhibited very weak activity (Figure 6).
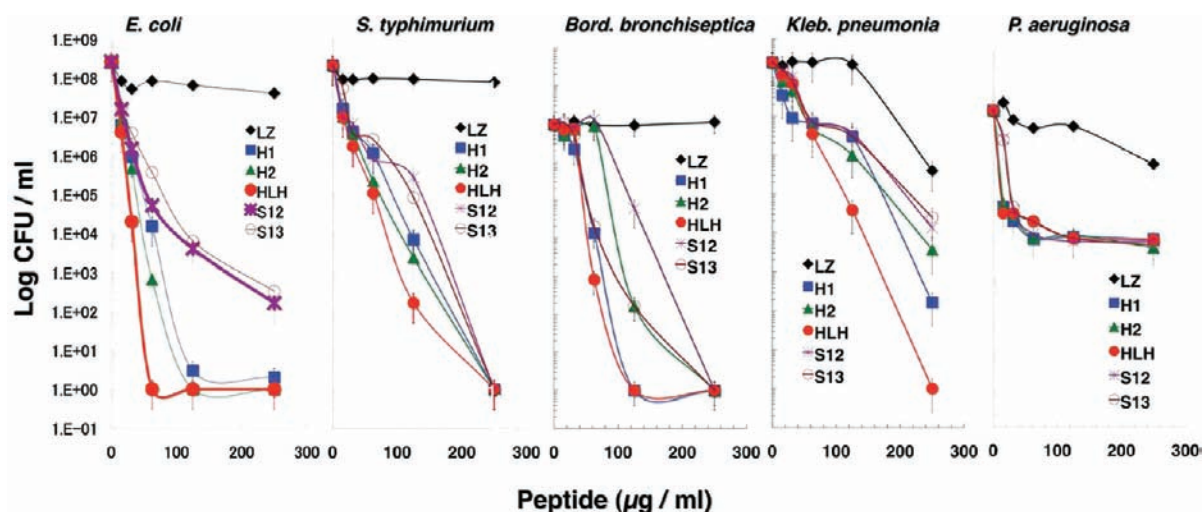
Figure 4. Bactericidal activity of the synthetic peptides of hLZ against Gram-negative bacteria. Activity was assessed against *E. coli* K-12, *Salmonella typhimurium*, *Bordetella bronchiseptica*, *Klebsiella pneumonieae*, and *Pseudomonas aeruginosa* at different doses of peptides or intact human lysozyme (LZ). The assays were performed in duplicates from four parallel wells per sample.

Figure 5. Bactericidal activity of the synthetic peptides of hLZ against Gram-positive bacteria. Activity was assessed against *Staphylococcus aureus*, *Staphylococcus epidermidis*, *Streptococcus zooepidemicus*, *Propionibacterium acnes*, and *Corynebacterium minutissimum* at different doses of peptides or intact human lysozyme (LZ). The assays were performed in duplicates from four parallel wells per sample.

Outer Membrane Disruption in Gram-Negative Bacteria. The ability of the peptides to permeabilize the OM of the Gram-negative *E. coli* K-12 and *Ps. aeruginosa* was assessed by measuring their ability to promote the uptake of 1-*N*-phenylnaphthylamine (NPN) into intact cells (Figure 7). NPN is completely quenched in aqueous environments, whereas in a hydrophobic environment, such as the interior of OM, it fluoresces strongly. Compared to the well-known OM-destabilizing antibiotic, polymyxin B (Plxn B), all of the peptide motifs, but not hLZ, were able to significantly facilitate, to variable degrees, the uptake of NPN, into the OM of both strains. The peptide concentration causing half the maximal uptake of NPN ranged from 4 to 5 μM in *E. coli* and from 7 to 9 μM in *Ps. aeruginosa* for each of the five peptides. The helical peptides (HLH, H1, and H2) and the helix—sheet

H2—S12 peptide displayed a progressive increase in NPN uptake, more pronounced than that of PlxB, in *E. coli* (Figure 7A), but all peptides exhibited weaker uptake than PlxB in *Ps. aeruginosa* (Figure 7B). The extent of NPN uptake increases as the amount of peptides increases to 14 μM; in contrast, there is no significant increase in NPN uptake by hLZ. Remarkably, the extent as well as the order of magnitude of NPN uptake by the peptides was different in *E. coli* K-12 and *Ps. aeruginosa*, which reflects microbe-specific disruption effect of each peptide motif.

Membrane Integrity in Gram-Negative and Gram-Positive Bacteria. To investigate whether the different antibacterial activities exerted by the peptide motifs of hLZ could be ascribed to different capacities of the peptides to permeabilize bacterial cells, the integrity of the cytoplasmic membrane was examined using
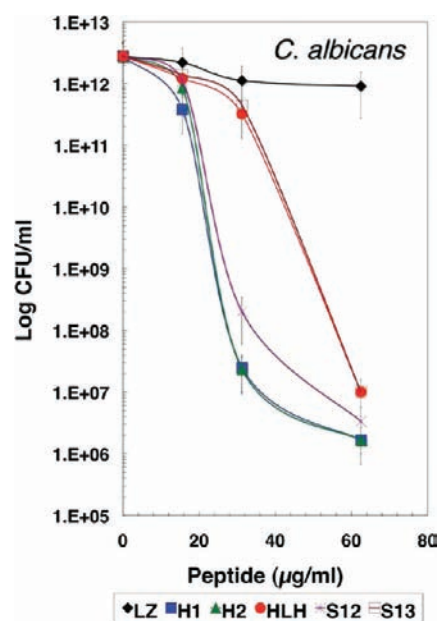
Figure 6. Bactericidal activity of the synthetic peptides of hLZ against *Candida albicans*. The assay was performed at different concentrations of peptides or intact human lysozyme (LZ) in duplicates from four parallel wells per sample.
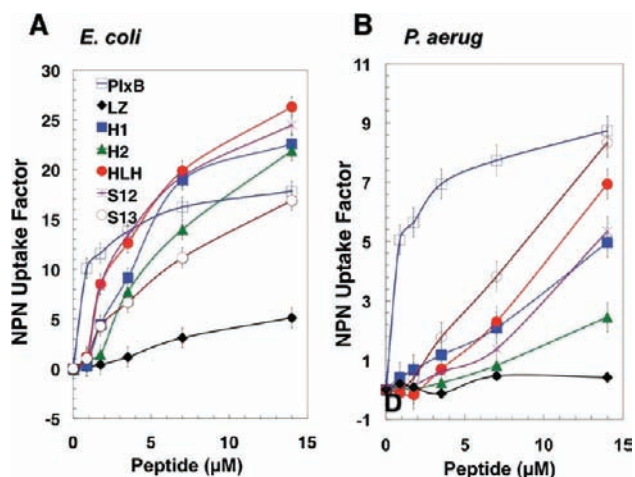

Figure 7. Dose—response curve of outer membrane (OM) perturbation by the synthetic peptides. OM permeabilization of *E. coli* K-12 (A) and *P. aeruginosa* (B) was monitored by fluorescence increase due to NPN partitioning into the OM. Samples were hLZ, synthetic peptides of hLZ, and the antibiotic polymyxin B, which served as a positive control. The results are expressed as NPN uptake factors as described under Materials and Methods. Values represent the mean of three independent experiments from four parallel wells per sample.

the fluorescent probe PI. PI incorporates and stains the nucleic acids only in cells with permeabilized membranes. When the parent HLH peptide was added to Gram-negative *E. coli* (Figure 8A) or Gram-positive *Staph. aureus* (Figure 8B) bacteria, there was a progressive increase in membrane permeabilization up to 60 min. The N-terminal helix (H1) of HLH showed an initial increase in PI-permeable *E. coli* up to 20 min followed by a steady state (Figure 8A), but exerted much less effect to *Staph. aureus* (Figure 8B). The C-terminal helix (H2) did not affect the

membrane integrity of both strains. The helix—sheet peptides H2—S13 had no effect on the membrane integrity of both strains (Figure 8), whereas H2—S12 exhibited a moderate time-dependent increase in PI-permeable cells only in the Gram-positive *Staph. aureus* (Figure 8B). Remarkably, HLH and H1 peptides exhibited strong membrane permeabilization in *E. coli*, even greater than that of the membrane-destabilizing agent PlxB, whereas the effect of hLZ was negligible (Figure 8A). For the Gram-positive *S. aureus*, hLZ caused the strongest loss of membrane integrity followed by HLH, PlxB, and then H2—S12, whereas the other peptides (H1, H2, and H2—S13) were almost inactive (Figure 8B). The effect of each peptide on the PI-permeable cells (Figure 8) does not correlate with their bactericidal potencies (Figures 4 and 5). The data suggest bacterial toxicity of each peptide occurs by a different mechanism that appears to range from pore formation to the blockage of proton motive force (respiration) through the membranes.

The results obtained from PI permeability assay indicate that the most potent bactericidal peptides (HLH and H1) instigate severe membrane damage in the membranes of Gram-negative bacteria (Figure 8A). In contrast, the cytoplasmic membrane damage induced in Gram-positive *Staph. aureus* by H1 peptide, as well as H2, H2—S12, and H2—S13 peptides, was not remarkable (Figure 8B). On the other hand, the NPN uptake assay demonstrated that the five synthetic peptides were able to induce, to different degrees, damage in the OM (Figure 7). Therefore, it is likely that the peptides exert their bactericidal effect by formation of transient pores in the cytoplasmic membrane of the target cell. These transient pores may be ion channels with different ion specificity, size, and duration of existence. Hence, it is not surprising that H1 and H2 peptides are highly bactericidal to *Staph. aureus* (Figure 5), but they do not induce PI permeability of cytoplasmic membrane in *Staph. aureus* (Figure 8B). This further indicates that the antimicrobial activity is not simply due to cell lysis through large pore formation. The specificity of the channels formed by the synthetic peptides can be evaluated further by elucidating their effect on transmembrane potentials in *Staph. aureus*.

Collapse of Transmembrane Potential in Gram-Positive Bacteria. The peptides were evaluated for their efficiency in collapsing the proton motive force (PMF), the electrochemical gradient essential for numerous cellular processes, mainly respiration.[42] The PMF consists of the transmembrane electrical potential ($\Delta\psi$) and the chemical pH gradient (ΔpH) provided by ions, basically to form metabolic energy such as ATP. The assay was conducted using the *Staph. aureus* cells in TSB medium consequently energized (hyperpolarized) through supplementation of valinomycin (a K$^+$ ionophore). The addition of the membrane potential sensitive fluorescent probe (DiSC$_3$) resulted in a sharp increase in fluorescence (Figure 9). When the $\Delta\psi$ was selectively energized with valinomycin (Val), the fluorescence intensity was sharply quenched as a result of the rapid intracellular localization of the DiSC$_3$ probe in exchange with K$^+$ ions. When the ΔpH was selectively reduced with nigericin (an electroneutral K$^+$/H$^+$ exchanger), the fluorescence intensity was gradually increased to reach maximum within 200 s (Figure 9, Nig). A gradual increase by Nig in the fluorescence intensity of the Val-energized cells, loaded with the potential-sensitive probe (DiSC$_3$), points to a complete collapse of the $\Delta\psi$ as a result of depolarization of the cellular cytoplasmic membranes.
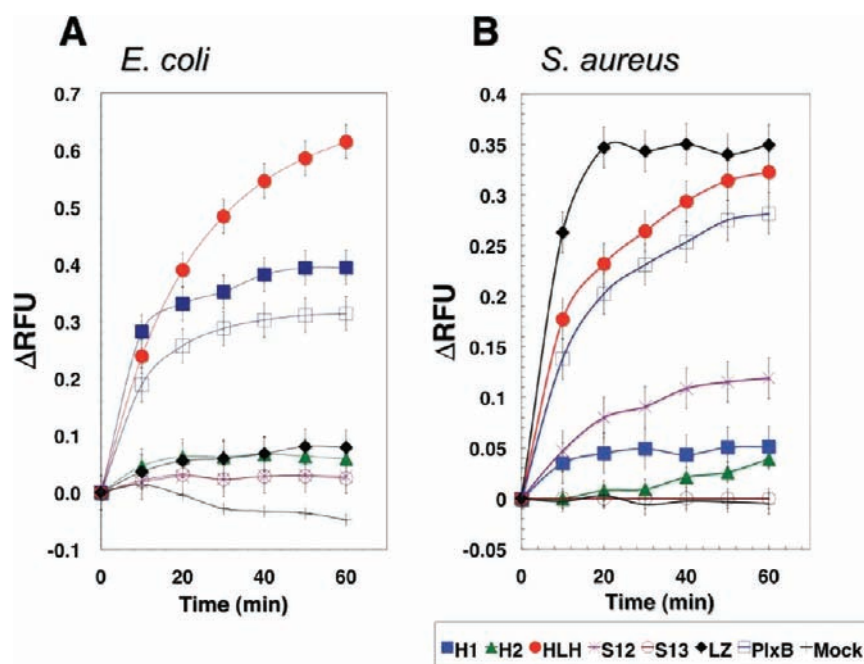
Figure 8. Cytoplasmic membrane (CM) disruption of *E. coli* K-12 (A) and *Staph. aureus* (B) was monitored by red fluorescence increase due to permeation of propidium iodide into the cells and subsequent binding to intracellular DNA. Samples were hLZ and its synthetic peptides, whereas the antibiotic polymyxin B served as a control. The results are expressed as changes in relative fluorescence unit (RFU) as a function of peptide concentration. Values represent the mean of three independent experiments from four parallel wells per sample.
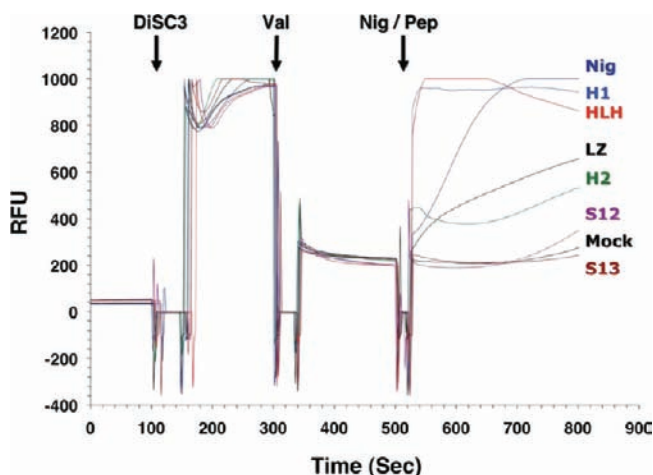
Figure 9. Collapse of bacterial membrane potential ($\Delta\psi$) of *Staph. aureus* by peptides of hLZ. Inhibition of $\Delta\psi$ was based on utilizing potential-sensitive dye $DiSC_3(5)$. Exponentially growing cells dispersed in potassium-free buffer were spiked with $5\,\mu M$ $DiSC_3$. Treatment of the cells with $5\,\mu M$ valinomycin (Val) causes a hyperpolarization of the membrane, due to the increased membrane permeability to K^+, resulting in diffusion of the dye into cells. When steady-state fluorescence levels were obtained, $3\,\mu L$ of peptide or hLZ ($14\,\mu M$) was added. Nigericin (Nig) was added ($2\,\mu M$), as a depolarizing positive ionophore, to collapse the potential through electroneutral exchange of K^+ ions. Mock cells were treated without peptide or ionophore. Arrows indicate the time at which ionophores or peptides were added to the live cells. Each curve is the average of three independent measurements (SD $\leq \pm8\%$).

The most potent bactericidal peptides (HLH and H1) induced complete collapse of the transmembrane electric potential ($\Delta\psi$) in *Staph. aureus* cells, as evidenced by a sharp increase in the fluorescence of the Val-energized cells (Figure 9). The H2 peptide and intact hLZ induced gradual collapse of the $\Delta\psi$, but to a slower and lesser extent than Nig. The helix–sheet H2–S12 peptide induced a very slow collapse of the $\Delta\psi$, whereas the H2–S13 peptide did not produce such an effect, similar to the negative control (Mock). Conditions of the experiment were selected so that the pH of the assay buffer would be higher (pH 7.4) than the intracellular pH. Consequently, a peptide-induced decrease in ΔpH, even sharper than that of Nig, further signifies the ability of the antimicrobial peptides to dissipate not only the $\Delta\psi$ but also the ΔpH of the target cell.

Remarkably, the bactericidal potency of each peptide against *Staph. aureus* (Figure 5) paralleled its ability to dissipate the transmembrane potential (Figure 9) as well as PI permeation of the cytoplasmic membrane (Figure 8). The results confirm the conclusion that although all peptides exhibit bactericidal activity, the highly potent peptides (HLH and H1) target the cytoplasmic membrane of the pathogen, whereas their precise mechanism of action is the depolarization of the membrane potential (respiration inhibition).

■ DISCUSSION

The antimicrobial peptides are frequently produced from a precursor protein in multiple structurally related isoforms with each isoform displaying differential antimicrobial activity, and it has been speculated that this molecular complexity is important in protecting the animal from invasion by an array of different microorganisms.[41] Recently, we showed that pepsin, under conditions relevant to the newborn stomach, cleaves cLZ at specific loops to generate five antimicrobial peptide motifs. However, the defense action of these individual peptides was neither investigated nor had been identified in hLZ, the actual

innate defense molecule in human milk. In this study, we investigated the spectrum of multiple structurally related synthetic peptide isoforms that could be proteolytically released from hLZ in the newborn stomach against a range of pathogenic microorganisms. Furthermore, we analyzed (a) whether the structural motifs (helix vs helix—sheet) play a role in the antimicrobial action of the hLZ-derived peptides, (b) whether these structurally different peptides of hLZ differ in their mode of interaction with bacterial membranes, and (c) whether the killing mechanism of the hLZ peptides is related to global membrane disintegration or the collapse of the vital transmembrane potential via ion channel formation, in order to explore the potential of these novel peptides in the treatment of infectious disease.

The main conclusion of this study is that testing the antimicrobial activity of synthetic peptides with multiple structural motifs of hLZ explored, for the first time, the presence of powerful bactericidal peptides within the N-terminal domain of hLZ and enabled the selection of peptides suitable for treatment of microbial infections. A significant correlation could be established between the in vitro antimicrobial potency and the structural motifs of the peptides (Figure 2). However, no significant relationship between the pI value of the peptide and its antimicrobial activity was observed, which indicates that the peptide conformation plays an important role rather than cationicity. This is confirmed by experiments with the helical motifs HLH (pI 9.24) and H1 (pI 10.05), which showed HLH is predominantly stronger against a range of pathogens (Figures 4 and 5), as well as with the helix—sheet motifs H2—S12 (pI 8.15) and H2—S13 (pI 9.04), whereas H2—S12 is significantly stronger against Staph. aureus (Figure 5) and Ca. albicans (Figure 6). Remarkably, in contrast to the peptide containing the β-sheet (H2—S12 and H2—S13), synthetic fragments comprising α-helix (HLH, H1, and H2) displayed the highest, dose-dependent antibacterial activity toward Gram-negative bacteria. Poor activity of the H2—S12 and H2—S13 peptides comprising the β-sheet may be attributed to low linear charge density and lipophilicity (Figure 2). The antimicrobial activity of the peptides containing the single α-helix (H1 and H2) was also seen against Ca. albicans, indicating that this domain plays an important role in the antimicrobial activity of hLZ toward a variety of pathogens. An explanation for this phenomenon is that the helical domain 3—38 seems to be responsible for binding to microorganisms, as it is surface exposed on the lysozyme molecule.

The five peptides of hLZ were able to permeabilize the outer membranes of both E. coli and Ps. aeruginosa (Figure 7). The antimicrobial potencies against Ps. aeruginosa of all peptides were almost similar in magnitude (Figure 4), but their abilities to permeabilize its OM differed greatly (Figure 7B). On the other hand, the helical peptides, HLH, H1, and H2, were much stronger than the helix—sheet peptides, H2—S12 and H2—S13, in killing E. coli (Figure 4), but H2—S12 was as potent as the helical peptides in permeabilizing its OM (Figure 7A). These results suggest that HLH, H1, H2, H2—S12, and H2—S13 are antimicrobial peptides with microbe-specific antimicrobial activities, whereas each peptide may embark on a different target on the microbial surface. The experiments of PI permeability showed that the most potent antimicrobial peptide, HLH, is able to permeabilize the cytoplasmic membranes of both Gram-negative (Figure 8A) and Gram-positive (Figure 8B) bacteria. The other potent antimicrobial helical peptide, H1, caused a remarkable permeabilization, comparable to that of HLH, of the cytoplasmic membrane of Gram-negative (Figure 8A), but was much less effective on the cytoplasmic membrane of Gram-

positive bacteria (Figure 8B). The other peptides, H2, H2—S12, and H2—S13, exhibited negligible effect on the cytoplasmic membrane of both bacteria (Figure 8), despite the marginal permeabilization caused by H2—S12 in Gram-positive Staph. aureus (Figure 8B).

It should be noted that the five peptides were effective in killing Staph. aureus (Figure 5) and E. coli (Figure 4) and possessed considerable ability to disrupt the OM of E. coli (Figure 7A). But all peptides, except the HLH peptide, exhibited a negligible effect on the cytoplasmic membrane of Staph. aureus (Figure 8B). When cytoplasmic membrane permeabilization was assessed by following the leakage of cFDA from labeled cells of Staph. aureus and E. coli K12 or by assessing the efflux of ONP$^+$ (hydrolyzed o-nitrophenyl-3-D-galactoside by the intracellular β-galactosidase) from E. coli K12, all peptides of hLZ blocked passage (efflux) through the membrane (data not shown). The results all together demonstrate that the helical peptide motifs of hLZ target the electrochemical membrane potential, rather than causing leakage of intracellular contents, of both Gram-positive and Gram-negative bacteria, obviously by interruption of PMF. The sharp depletion of transmembrane potential ($\Delta\psi$ or ΔpH) induced by the helical HLH or H1 peptides was total, evident by the fact that treatment with the ionophore Nig (used to dissipate any residual PMF) did not lead to any additional increase in fluorescence intensity, whereas H2 peptide and intact hLZ caused slower dissipation (Figure 9). However, for the helix—sheet peptide motifs, H2—S12 and H2—S13, the membrane depolarization was not enough to cause cell death; instead, it appeared to be an intermediate step in the process. The helix—sheet peptides probably interacted with the bacterial membranes and killed the target bacteria by progressive disruption of bacterial membranes or interfering with yet unknown biological processes. This finding is consistent with the theory that the higher level of membrane depolarization caused by the helical peptides of hLZ leads to the loss of the proton gradient, resulting in rapid cell death. These peptides of hLZ showed faster killing kinetics against Gram-negative, Gram-positive, and fungal C. albicans than the intact hLZ. The enhanced killing activities are due to increased binding and penetration into cell membranes, whereas the helical motifs specifically targeted bacterial respiration.

Regardless of the significant scientific finding of novel bactericidal peptides in hLZ, this work lays a foundation for generating smart antimicrobial peptides to complement currently available conventional antibiotics. This finding indicates that there are a variety of peptides within the sequence of hLZ that are able to fight infections in the infant gastrointestinal tract and that these peptides use at least two different mechanisms of action (dissipation of bacterial respiration and loss of membrane integrity). The use of peptides with different mechanisms may be advantageous in decreasing the likelihood of resistance and promoting synergistic interactions. This finding also indicates that if a mixture of antimicrobial peptides is isolated from hLZ and used in therapeutic applications, peptides utilizing different mechanisms should be present to provide "insurance" of the product's effectiveness against a wide range of pathogens. Although the strongest antibacterial activity is observed for the helix—loop—helix peptide (HLH, residues 1—38), the high costs to synthesize this peptide and the elaborating purification procedures to obtain the natural HLH 1—38 from hLZ may limit its use for treatment of infectious diseases. In this respect, a selected synthetic peptide, comprising the potent microbicidal

N-terminal helix (H1, residues 1—17) of the HLH domain, offers a promising alternative. Its ease of synthesis, as well as its strong antimicrobial activity toward a wide spectrum of microorganisms, makes this peptide a promising natural candidate for antimicrobial therapy against microbial infections in man.

■ AUTHOR INFORMATION

Corresponding Author

*Phone: +81 (99) 285-8656. Fax: +81 (99) 285-8525. E-mail: hishamri@chem.agri.kagoshima-u.ac.jp.

■ ACKNOWLEDGMENT

■ ABBREVIATIONS USED

hLZ, human lysozyme; cLZ, chicken egg-white lysozyme; HLH, helix—loop—helix; H1 and H2, helix-1 and helix-2 of human lysozyme sequence; H2—S12 or H2—S13, helix-2 extended with two β-strands or three β-strands of human lysozyme sequence; CFU, colony-forming units; diS-C3-(5), 3,3′-diisopropylthiadicarbocyanine iodide; Val, valinomycin; Nig, nigericin; NPN, N-phenyl-1-naphthylamine; PI, propidium iodide; OM, outer membrane; IM, inner membrane; β-ME, 2-mercaptoethanol; tricine-SDS-PAGE, tricine sodium dodecyl sulfate polyacrylamide gel electrophoresis; ESI-MS-MS, electrospray ionization tandem mass spectrometry.

■ REFERENCES

(1) Jolles, P.; Jolles, J. What's new in lysozyme research? Always a model system, today as yesterday. *Mol. Cell. Biochem.* **1984**, *63*, 165–189.

(2) Banks, J. G.; Board, R. G.; Sparks, N. H. Natural antimicrobial systems and their potential in food preservation of the future. *Biotechnol. Appl. Biochem.* **1986**, *8*, 103–147.

(3) Hung, S. C.; Wang, W.; Chan, S. I.; Chen, H. M. Membrane lysis by the antibacterial peptides cecropins B1 and B3: a spin-label electron spin resonance study on phospholipid bilayers. *Biophys. J.* **1999**, *77*, 3120–3133.

(4) Bjermer, L.; Back, O.; Roos, G.; Thunell, M. Mast cells and lysozyme positive macrophages in bronchoalveolar lavage from patients with sarcoidosis. Valuable prognostic and activity marking parameters of disease. *Acta Med. Scand.* **1986**, *220*, 161–166.

(5) Lemarbre, P.; Rinehart, J. J.; Kay, N. E.; Vesella, R.; Jacobs, H. S. Lysozyme enhances monocyte-mediated tumoricidal activity: a potential amplifying mechanism of tumor killing. *Blood* **1981**, *58*, 994–999.

(6) Sava, G.; Benetti, A.; Ceschia, V.; Pacor, S. Lysozyme and cancer: role of exogenous lysozyme as anticancer agent (review). *Anticancer Res.* **1989**, *9*, 583–591.

(7) Hasselberger, F. X. *Uses of Enzymes and Immobilized Enzymes*; Nelson-Hall: Chicago, IL, 1978; p 128.

(8) Ibrahim, H. R.; Aoki, T.; Pellegrini, A. Strategies for new antimicrobial proteins and peptides: lysozyme and aprotinin as model molecules. *Curr. Pharm. Des.* **2002**, *8*, 671–693.

(9) Schindler, M.; Assaf, Y.; Sharon, N.; Chipman, D. M. Mechnism of lysozyme catalysis: role of the ground-state strain in subsite D in hen-egg white and human lysozymes. *Biochemistry* **1977**, *16*, 423–431.

(10) Hankiewicz, J.; Swierczek, E. Lysozyme activity in various human body fluids. *Clin. Chem. Acta* **1974**, *57*, 205–209.

(11) Venge, P.; Foucard, T.; Henriksen, J.; Hakansson, L.; Kreuger, A. Serum-levels of lactoferrin, lysozyme and myeloperoxidase in normal, infection-prone and leukemic children. *Clin. Chim. Acta* **1984**, *136*, 121–130.

(12) Ibrahim, H. R. On the novel catalytically-independent antimicrobial function of hen egg-white lysozyme: a conformation-dependent activity. *Nahrung* **1998**, *42*, 187–193.

(13) Ibrahim, H. R.; Higashiguchi, S.; Juneja, L. R.; Kim, M.; Yamamoto, T. A structural phase of heat-denatured lysozyme with novel antimicrobial action. *J. Agric. Food Chem.* **1996**, *44*, 1416–1423.

(14) Ibrahim, H. R.; Matsuzaki, T.; Aoki, T. Genetic evidence that antibacterial activity of lysozyme is independent of its catalytic function. *FEBS Lett.* **2001**, *506*, 27–32.

(15) Ibrahim, H. R.; Thomas, U.; Pellegrini, A. A helix-loop-helix peptide at the upper lip of the active site cleft of lysozyme confers potent antimicrobial activity with membrane permeabilization action. *J. Biol. Chem.* **2001**, *276*, 43767–43774.

(16) Irwin, D. M.; Prager, E. M.; Wilson, A. C. Evolutionary genetics of ruminant lysozymes. *Anim. Genet.* **1992**, *23*, 193–202.

(17) Flescher, E.; Keisari, Y.; Lengy, J.; Gold, D. On the possible schistosomulicidal effect of macrophage-derived lysozyme. *Parasitology* **1991**, *103*, 161–164.

(18) Gibson, K. F.; Phadke, S. Intracellular distribution of lysozyme in rat alveolar type II epithelial cells. *Exp. Lung Res.* **1994**, *20*, 595–611.

(19) Lehrer, R. I.; Ganz, T. Antimicrobial polypeptides of human neutrophils. *Blood* **1990**, *76*, 2169–2181.

(20) Ridder, A. N. J. A. Analysis of the role of interfacial tryptophan residues in controlling the topology of membrane proteins. *Biochemistry* **2000**, *39*, 6521–6528.

(21) Thompson, A. B.; Bohling, T.; Payvandi, F.; Rennard, S. I. Lower respiratory tract lactoferrin and lysozyme arise primarily in the airways and are elevated in association with chronic bronchitis. *J. Lab. Clin. Med.* **1990**, *115*, 148–158.

(22) Travis, S. M.; Conway, B. A.; Zabner, J.; Smith, J. J.; Anderson, N. N.; Singh, P. K.; Greenberg, E. P.; Welsh, M. J. Activity of abundant antimicrobials of the human airway. *Am. J. Respir. Cell Mol. Biol.* **1999**, *20*, 872–879.

(23) Throne, K. J. I.; Oliver, R. C.; Barrett, A. J. Lysis and killing of bacteria by lysosomal proteinases. *Infect. Immun.* **1976**, *14*, 555–563.

(24) Benes, P.; Koelsch, G.; Dvorak, B.; Fusek, M.; Vetvicka, V. Detection of procathepsin D in rat milk. *Comp. Biochem. Physiol.* **2002**, *133*, 113–118.

(25) Black, C. M.; Paliescheskey, M.; Beaman, B. L.; Donovan, R. M.; Goldstein, E. Modulation of lysosomal protease—esterase and lysozyme in Kupffer cells and peritoneal macrophages infected with *Nocardia asteroides*. *Infect. Immun.* **1986**, *54*, 917–919.

(26) Coonrod, J. D. The role of extracellular bactericidal factors in pulmonary host defense. *Semin. Respir. Infect.* **1986**, *1*, 118–129.

(27) McClellan, K. A. Mucosal defense of the outer eye. *Surv. Ophthalmol.* **1997**, *42*, 233–246.

(28) Sathe, S.; Sakata, M.; Beaton, A. R.; Sack, R. A. Identification, origins and the diurnal role of the principal serine protease inhibitors in human tear fluid. *Curr. Eye Res.* **1998**, *17*, 348–362.

(29) Ellison, R. T., 3rd; Giehl, T. J. Killing of Gram-negative bacteria by lactoferrin and lysozyme. *J. Clin. Invest.* **1991**, *88*, 1080–1091.

(30) Nascimento de Araujo, A.; Giugliano, L. G. Human milk fractions inhibit the adherence of diffusely adherent *Escherichia coli* (DAEC) and enteroaggregative *E. coli* (EAEC) to HeLa cells. *FEMS Microbiol. Lett.* **2000**, *184*, 91–94.

(31) Kohler, H.; Donarski, S.; Stocks, B.; Parret, A.; Edwards, C.; Schroten, H. Antibacterial characteristics in the feces of breast-fed and formula-fed infants during the first year of life. *J. Pediatr. Gastroenterol. Nutr.* **2002**, *34*, 188–193.

(32) Caputo, E.; Manco, G.; Mandrich, L.; Guardiola, J. A novel aspartyl proteinase from apocrine epithelia and breast tumors. *J. Biol. Chem.* **2000**, *275*, 7935–7941.

10344

dx.doi.org/10.1021/jf2020396 |*J. Agric. Food Chem.* 2011, 59, 10336–10345

(33) Hooper, N. M. *Proteases in Biology and Medicine*; Portland Press: London, U.K., 2002.

(34) Kageyama, T. Pepsinogens, progastricsins, and prochymosins: structure, function, evolution, and development. *Cell. Mol. Life Sci.* **2002**, *59*, 288–306.

(35) Ichinose, M.; Miki, K.; Furihata, C.; Tatematsu, M.; Ichihara, Y.; Ishihara, T. DNA methylation and expression of the rat pepsinogen gene in embryonic, adult, and neoplastic tissues. *Cancer Res.* **1988**, *48*, 1603–1609.

(36) Lee-Huang, S.; Huang, P.; Sun, Y.; Kung, H. F.; Blithe, D. L.; Chen, H. C. Lysozyme and RNases as anti-HIV components in β-core preparations of human chorionic gonadotropin. *Proc. Natl. Acad. Sci. U.S. A.* **1999**, *96*, 2678–2681.

(37) Ibrahim, H. R.; Inazaki, D.; Abdou, A.; Aoki, T.; Kim, M. Processing of lysozyme at distinct loops by pepsin: a novel action for generating multiple antimicrobial peptide motifs in the newborn stomach. *Biochim. Biophys. Acta* **2005**, *1726*, 102–114.

(38) Helander, I. M.; Sandholm, T. M. Fluorometric assessment of Gram-negative bacterial permeabilization. *J. Appl. Microbiol.* **2000**, *88*, 213–219.

(39) Bolscher, J. G. M.; Van der Kraan, M. I. A.; Nazmi, K.; Kalay, H.; Grün, C. H.; Van't Hof, W.; Veerman, E. C. I.; Amerongen, A. V. N. A one-enzyme strategy to release an antimicrobial peptide from the LFampin-domain of bovine lactoferrin. *Peptides* **2006**, *27*, 1–9.

(40) Sims, P. J.; Waggoner, A. S.; Wang, C. H.; Hoffman, J. F. Studies on the mechanism by which cyanine dyes measure membrane potential in red blood cells and phosphatidylcholine vesicles. *Biochemistry* **1974**, *13*, 3315–3330.

(41) Mor, A.; Hani, K.; Nicolas, P. The vertebrate peptide antibiotics dermaseptins have overlapping structural features but target specific microorganisms. *J. Biol. Chem.* **1994**, *269*, 31635–31641.

(42) Montville, T. J.; Bruno, M. E. Evidence that dissipation of proton motive force is a common mechanism of action for bacteriocins and other antimicrobial proteins. *Int. J. Food Microbiol.* **1994**, *24*, 53–74.